Research Square

Preprints are preliminary reports that have not undergone peer review.
They should not be considered conclusive, used to inform clinical practice,
or referenced by the media as validated information.

Digitizing Eyelid Contour: Image-Derived Geometric Biomarkers for Objective Ptosis Severity Assessment

Elias Khalili Pour
Farabi Hospital
Yasaman Sadeghi
Farabi Hospital
Hamid Riazi-Esfahani
Farabi Hospital
Tahereh Mahmoudi
Shiraz University of Medical Sciences
Kamran Rezaei
Shahid Beheshti University of Medical Sciences
Samin Khannejad
Shahid Beheshti University of Medical Sciences
Kimia Vakili
Shahid Beheshti University of Medical Sciences
Sajad Mansourian
Farabi Hospital
Seyed Mohsen Rafizadeh
Mohsen_raf1354@yahoo.com

Farabi Hospital

Article

Keywords: Blepharoptosis, Eyelid Contour, Margin Reflex Distance 1 (MRD1), Upper Nasal Index (UNI), Upper Temporal Index (UTI), Upper Lid Contour Circularity Index (ULCCI), Diagnostic Image Processing

Posted Date: November 10th, 2026

DOI: https://doi.org/10.21203/rs.3.rs-11103495/v1

License: This work is licensed under a Creative Commons Attribution 4.0 International License. Read Full License

Additional Declarations: No competing interests reported.

Abstract

Purpose

To introduce and evaluate three novel two-dimensional (2D) geometric eyelid contour indices—Upper Nasal Index (UNI), Upper Temporal Index (UTI), and Upper Lid Contour Circularity Index (ULCCI)—for objective blepharoptosis severity assessment, bridging expert clinical impression with traditional margin reflex distance 1 (MRD1)-based classification.

Methods

This cross-sectional study evaluated 94 eyes from 94 participants (eyes stratified into control/no ptosis, mild, moderate, and severe groups) using both expert clinical grading (holistic visual impression) and standard MRD1 measurements. Standardized full-face digital photographs were processed using MATLAB to calculate 2D area-derived regional indices (UNI and UTI) and ULCCI, defined as the ratio of upper eyelid contour length to the circumference of the upper half of a reference circle. Group differences were assessed using generalized linear models, including analyses adjusted for age and sex, and diagnostic performance was evaluated using ROC curve analysis.

Results

Expert clinical grading demonstrated substantial agreement with MRD1 classification (weighted Cohen's κ = 0.775, 95% CI 0.695–0.855) and showed excellent reliability (interobserver ICC = 0.92; intraobserver ICC = 0.93). All three indices significantly differentiated overall severity groups under both classification frameworks after adjustment for age and sex (all $P < 0.001$). UNI demonstrated the greatest numerical AUC for differentiating no ptosis from mild ptosis in both expert clinical grading (AUC = 0.768) and MRD1-based classification (AUC = 0.846). UTI demonstrated the greatest numerical AUC for differentiating moderate from severe ptosis using MRD1-based classification (AUC = 0.817), while ULCCI showed the greatest numerical AUC under expert clinical grading for this comparison (AUC = 0.744).

Conclusions

Novel 2D geometric indices provide objective quantitative measures of eyelid contour that complement conventional central MRD1 assessment. UNI showed particular utility in distinguishing early ptotic changes, whereas UTI quantified advanced temporal contour changes and ULCCI reflected global contour characteristics that contribute to expert clinical assessment. Together, these digital biomarkers provide a reproducible framework for quantitative eyelid phenotyping and may support future scalable image-based diagnostic documentation, automated assessment workflows, and computational approaches to personalized ophthalmic care.

Introduction

Blepharoptosis is characterized by an abnormal downward displacement of the upper eyelid. In adults, the upper eyelid margin normally rests approximately 0.5–2 mm below the superior corneal limbus and typically overlies the superior cornea to the level of the upper pupillary border.(1) Blepharoptosis may be congenital or acquired and can occur unilaterally or bilaterally.(1, 2) The condition most commonly results from dysfunction of the levator palpebrae superioris muscle, its aponeurosis, or Müller's muscle, although neurogenic disorders may also impair eyelid elevation.(1)

Beyond its functional and cosmetic impact, blepharoptosis can affect the cornea, ocular surface, and anterior segment.(3) Previous studies have demonstrated that ptosis and its surgical correction may induce significant changes in corneal topography, refractive status, and astigmatism.(4, 5) More recently, alterations in corneal epithelial thickness profiles, particularly superior epithelial thinning, have been reported in ptotic eyes.(6, 7) Furthermore, ptosis correction has been associated with postoperative changes in keratometric measurements and intraocular lens power calculations.(8) These findings underscore the importance of accurately assessing eyelid position and morphology in patients with blepharoptosis.

The clinical evaluation of blepharoptosis primarily relies on measurements such as margin reflex distance 1 (MRD1), palpebral fissure height (PFH), and levator muscle function (LMF). MRD1 and PFH are widely used to quantify ptosis severity, whereas LMF is essential for surgical planning and selection of the appropriate corrective procedure. (9)The primary goal of ptosis surgery commonly entails achieving an increased MRD1, which represents the central height of the upper eyelid and is partly dependent on examiner technique and measurement.(10, 11) However, these measurements provide limited information regarding eyelid contour. In particular, MRD1 reflects only the central height of the upper eyelid and does not capture contour abnormalities such as notching, temporal flare, or displacement of the eyelid peak.(12–15) Moreover, previous studies have reported limited repeatability and reproducibility of MRD1 measurements.(16, 17) Because eyelid contour contributes substantially to both functional and aesthetic outcomes, objective assessment of contour is important for identifying morphological abnormalities, planning surgery, and evaluating postoperative outcomes.

Although MRD1 is the most widely used quantitative measure of ptosis severity, clinicians frequently consider additional morphological features, particularly eyelid contour, when assessing disease severity in routine practice. Consequently, expert clinical grading may not always correspond directly to MRD1 measurements. Evaluating quantitative eyelid contour indices using both expert clinical assessment and MRD1-based classification may therefore provide complementary information regarding their clinical utility and their ability to objectively characterize blepharoptosis severity.

Abnormal eyelid contour following ptosis surgery has been associated with visual field disturbances, cosmetic concerns, and ocular surface disorders.(3, 9) Accordingly, recent advances in ptosis surgery have emphasized achieving a more natural and symmetric eyelid contour.(18) This has stimulated interest in quantitative analysis of eyelid contour, and several image-based methods have been proposed to characterize eyelid morphology.(19–23) Nevertheless, assessment of eyelid contour in clinical practice and evaluation of surgical outcomes continue to rely largely on subjective grading systems, with outcomes commonly categorized as excellent, good, or acceptable.(14, 20, 24) Objective quantitative methods capable of distinguishing different degrees of ptosis severity remain limited.

Recent advances in medical image analysis have demonstrated the potential of digital approaches to extract clinically meaningful morphological features from routinely acquired images. However, clinically applicable

digital biomarkers for upper eyelid contour abnormalities remain insufficiently developed. A quantitative framework that captures regional and global eyelid contour characteristics may provide complementary information to conventional measurements and establish a foundation for future automated image-based clinical assessment.

Therefore, the present study introduces three image-derived quantitative upper eyelid contour indices—the Upper Nasal Index (UNI), Upper Temporal Index (UTI), and Upper Lid Contour Circularity Index (ULCCI). We evaluated their ability to objectively differentiate blepharoptosis across four severity grades using both expert clinical grading and MRD1-based classification and compared their diagnostic performance using receiver operating characteristic (ROC) analysis. By comparing these complementary classification approaches, we sought to determine which quantitative indices best reflect clinically perceived ptosis severity and which most closely correspond to MRD1-defined disease severity.

Materials and Methods

Study Design

This cross-sectional study was conducted at Farabi Eye Hospital, Tehran, Iran. The study protocol was approved by the Institutional Review Board and Ethics Committee of Tehran University of Medical Sciences (IR.TUMS.FARABIH.REC.1400.057) and adhered to the tenets of the Declaration of Helsinki. Written informed consent was obtained from all participants or their legal guardians.

The study evaluated quantitative upper eyelid contour indices in patients with unilateral blepharoptosis and healthy controls. Individuals aged ≥ 3 years with unilateral upper eyelid ptosis were eligible for inclusion. Exclusion criteria included previous eyelid surgery, orbital or eyebrow disorders, strabismus, eyelid abnormalities unrelated to ptosis (e.g., thyroid eye disease or facial nerve palsy), and botulinum toxin injection within the preceding six months.

The control group consisted of individuals without ocular or orbital abnormalities. For control participants, one eye was randomly selected for analysis.

Image Acquisition and MRD1 Measurement

Standardized full-face digital photographs were obtained using a Nikon D7500 camera equipped with an 18–140 mm VR AF-S DX lens (Nikon Corporation, Tokyo, Japan). Images were captured with participants seated upright in primary gaze. The camera was positioned at pupil level and maintained at a fixed distance of 25 cm from the participant.

Uncropped facial photographs were independently reviewed by three ophthalmologists (S.M.R., H.R.E., and E.K.P.), who graded ptosis severity based on the overall clinical appearance of the eyelid, including eyelid position, contour, and pupil coverage, without access to MRD1 measurements. Each ophthalmologist independently classified the ptotic eyes as having mild, moderate, or severe ptosis. The independent pre-consensus ratings were used to assess interobserver reliability. For assessment of intraobserver reliability, repeated independent ratings by the same observer were used. After completion of the reliability assessments,

discrepancies among observers were resolved by consensus, and the resulting consensus grade was used as the final expert clinical classification.

MRD1 was measured independently by two ophthalmologists using ImageJ software (National Institutes of Health, Bethesda, MD, USA). Following digital magnification of the photographs, a vertical line was drawn from the upper eyelid margin to the corneal light reflex. Measurements were recorded to the nearest 0.1 mm, and the mean of the two measurements was used for analysis.

Based on the mean MRD1 value, all analyzed eyes, including those from the separately selected control group, were independently categorized into four severity groups: no ptosis (MRD1 ≥ 4 mm), mild ptosis (MRD1 3 to < 4 mm), moderate ptosis (MRD1 1 to < 3 mm), and severe ptosis (MRD1 < 1 mm).

Image Processing and Eyelid Contour Analysis

Eyelid contour analysis was performed using MATLAB R2019 (MathWorks, Natick, MA, USA). Images were converted to grayscale and enhanced using homomorphic filtering and normalization techniques. The palpebral fissure region was isolated, and the medial and lateral canthi were manually marked by the operator.

A region of interest (ROI) encompassing the palpebral fissure was generated using an interactive polygonal tracing method. Tracing was initiated at one canthus, continued along the eyelid margin, and completed at the opposite canthus. The image was subsequently binarized, and an imaginary circle encompassing the eye was constructed using the line connecting the medial and lateral canthi as its diameter (Fig. 1).

Definition of Eyelid Contour Indices

An imaginary circle was constructed using the line connecting the medial and lateral canthi as its diameter (Fig. 2).

Upper Nasal Index (UNI): UNI was calculated as the ratio of the area enclosed between the upper eyelid margin and the diameter of the imaginary circle to the area of the upper nasal half of the circle. The nasal and temporal halves were defined by a perpendicular line passing through the midpoint of the circle diameter (Fig. 2A).

Upper Temporal Index (UTI): UTI was calculated using the same method as UNI but within the temporal half of the circle (Fig. 2B).

Upper Lid Contour Circularity Index (ULCCI): ULCCI was calculated as the ratio of the length of the upper eyelid contour to the circumference of the upper half of the imaginary circle (Fig. 2C).

Preparation of Schematic Illustrations of Eyelid Contour Analysis

Figures 7–9 were prepared as schematic illustrations to demonstrate the geometric principles underlying upper eyelid contour analysis. The synthetic eye images incorporated into these figures were generated using artificial intelligence (AI) tools, including Claude (Opus 5; Anthropic, San Francisco, CA, USA) and Google AI Studio (Nano Banana 2; Google, Mountain View, CA, USA); no patient photographs were used in their creation. The eyelid contours, geometric overlays, annotations, and displayed numerical values were constructed based on the

methodology and results of the present study. Figures were assembled and annotated using Adobe Illustrator and Adobe Photoshop (version 2025; Adobe, San Jose, CA, USA). Generative AI was not used to generate, modify, or analyze study data. All figures were reviewed and verified by the authors.

Statistical Analysis

Statistical analyses were performed using SPSS version 25.0 (IBM Corp., Armonk, NY, USA). Continuous variables are presented as mean ± standard deviation (SD), Categorical variables were presented as frequencies and percentages. Differences in categorical variables among severity groups were assessed using chi-square tests or Fisher's exact tests, as appropriate.

Comparisons of UNI, UTI, and ULCCI among severity groups were performed separately according to expert clinical grading and MRD1-based classification. Continuous eyelid contour indices were analyzed using generalized linear models with adjustment for age and sex to evaluate their independent association with ptosis severity classification. A Gaussian distribution with an identity link function was used for continuous outcomes. Pairwise comparisons between adjacent severity groups were performed with Sidak correction for multiple comparisons.

Agreement between expert clinical grading and MRD1-based classification was assessed using weighted Cohen's kappa coefficient with 95% confidence intervals (CIs). The interobserver and intraobserver reliability of expert clinical grading were evaluated using intraclass correlation coefficients (ICCs).

Receiver operating characteristic (ROC) curve analysis was performed to evaluate the diagnostic performance of UNI, UTI, and ULCCI for discriminating between adjacent severity categories: no ptosis versus mild ptosis, mild versus moderate ptosis, and moderate versus severe ptosis. Analyses were performed separately according to expert clinical grading and MRD1-based classification. The area under the ROC curve (AUC) was calculated with its corresponding 95% CI. For each ROC analysis, the optimal cutoff value was determined using the Youden index (J = sensitivity + specificity − 1), with the cutoff maximizing the Youden index considered the optimal threshold. Sensitivity and specificity at the optimal cutoff were reported.

The relationships between MRD1 and each of the three eyelid contour indices (UNI, UTI, and ULCCI) were assessed using Pearson correlation coefficients. Scatterplots with fitted linear regression trendlines were generated to visualize these relationships.

A two-sided P value < 0.05 was considered statistically significant.

Results

The expert clinical classification included 21 eyes with mild ptosis, 25 with moderate ptosis, and 18 with severe ptosis. The control group comprised 30 eyes from participants without ptosis.

Based on MRD1 measurements, 20 eyes were categorized as no ptosis, 24 as mild ptosis, 36 as moderate ptosis, and 14 as severe ptosis. Overall, there were no marked differences in the distribution of sex or laterality among the severity groups. The demographic and clinical characteristics of the study population according to expert clinical grading are summarized in Table 1, whereas the corresponding characteristics based on MRD1 classification are presented in Supplementary Table S1.

Expert clinical grading demonstrated substantial agreement with MRD1-based classification (weighted Cohen's κ = 0.775, 95% confidence interval [CI], 0.695–0.855; *P* < 0.001). Based on the independent pre-consensus ratings, expert clinical grading demonstrated high reliability, with an interobserver ICC of 0.92 and an intraobserver ICC of 0.93.

The mean values of UNI, UTI, and ULCCI according to expert clinical grading and MRD1-based classification are presented in Tables 2 and 3, respectively. Values are presented as unadjusted mean ± SD, while statistical comparisons were performed using generalized linear models adjusted for age and sex. After adjustment, significant overall differences among the four severity groups remained for all three indices under both classification methods (all *P* < 0.001).

Pairwise comparisons between adjacent severity groups after adjustment for age and sex are presented in Table 4.

Under expert clinical grading, UNI significantly differentiated all adjacent severity groups except the moderate versus severe comparison after adjustment. UTI significantly differentiated mild from moderate and moderate from severe ptosis but did not significantly differentiate control from mild ptosis. ULCCI significantly differentiated all adjacent severity groups (all *P* < 0.05).

Using MRD1-based classification, UNI and UTI each significantly differentiated all adjacent severity groups (no ptosis vs. mild, mild vs. moderate, and moderate vs. severe) (all *P* < 0.05), whereas ULCCI did not significantly differentiate no ptosis from mild ptosis.

Examination of the mean UNI and UTI values demonstrated a characteristic sequential pattern across ptosis severity using both expert clinical grading and MRD1-based classification. In eyes without ptosis, the two indices were nearly identical (expert grading: UTI 0.4216 ± 0.0553 vs. UNI 0.4273 ± 0.0370; MRD1 classification: UTI 0.4410 ± 0.0532 vs. UNI 0.4389 ± 0.0357), reflecting a relatively similar nasal and temporal contour proportions. In mild ptosis, UNI decreased more markedly than UTI (expert grading: UNI 0.3794 ± 0.0482 vs. UTI 0.4018 ± 0.0351; MRD1 classification: UNI 0.3796 ± 0.0428 vs. UTI 0.3904 ± 0.0405), indicating that early contour changes predominantly involve the nasal upper eyelid. In moderate ptosis, the values of UNI and UTI became comparable (expert grading: UNI 0.3388 ± 0.0363 vs. UTI 0.3347 ± 0.0364; MRD1 classification: UNI 0.3536 ± 0.0466 vs. UTI 0.3483 ± 0.0419), suggesting relatively uniform involvement of both eyelid regions. In severe ptosis, however, UTI decreased to a greater extent than UNI (expert grading: UTI 0.2829 ± 0.0691 vs. UNI 0.3018 ± 0.0726; MRD1 classification: UTI 0.2677 ± 0.0704 vs. UNI 0.2907 ± 0.0778), demonstrating disproportionately greater temporal eyelid descent in advanced disease. This sequential pattern was remarkably consistent across both classification methods.

Scatterplot analysis demonstrated significant positive correlations between MRD1 and all three eyelid contour indices (Fig. 3). MRD1 showed a strong positive correlation with UTI (r = 0.811, P < 0.001), followed by UNI (r = 0.726, P < 0.001) and ULCCI (r = 0.669, P < 0.001).

All three indices demonstrated an overall linear relationship with MRD1, with lower index values generally corresponding to lower MRD1 values and increasing ptosis severity.

The diagnostic performance of the three quantitative eyelid contour indices was further evaluated using ROC curve analysis, with results summarized in Table 5. For each comparison, the AUC, 95% confidence interval,

optimal cutoff determined by the Youden index, sensitivity, and specificity were calculated.

For differentiating no ptosis from mild ptosis, UNI demonstrated the highest AUC among the three indices under both expert clinical grading and MRD1-based classification, with AUCs of 0.768 (95% CI, 0.634–0.902) and 0.846 (95% CI, 0.733–0.959), respectivelyUnder expert clinical grading, the optimal UNI cutoff was 0.395, yielding a sensitivity of 62% and specificity of 87%. Under MRD1-based classification, the optimal cutoff was 0.423, with a sensitivity of 88% and specificity of 75%.

For differentiating mild from moderate ptosis, UTI achieved the highest AUC under expert clinical grading (0.918; 95% CI, 0.836–1.000), with an optimal cutoff of 0.362, sensitivity of 84%, and specificity of 90%. Under MRD1-based classification, ULCCI demonstrated the highest AUC (0.843; 95% CI, 0.744–0.942), with an optimal cutoff of 0.751, sensitivity of 75%, and specificity of 79%.

For differentiating moderate from severe ptosis, ULCCI had the highest AUC under expert clinical grading (AUC = 0.744; 95% CI, 0.582–0.906), with an optimal cutoff of 0.728, sensitivity of 61%, and specificity of 92%. Under MRD1-based classification, UTI showed the highest AUC (0.817; 95% CI, 0.676–0.959), with an optimal cutoff of 0.266, sensitivity of 57%, and specificity of 100%.

Overall, UNI showed particularly good discrimination between no ptosis and mild ptosis

whereas UTI and ULCCI demonstrated greater discriminatory ability for differentiating more advanced stages of ptosis, depending on the classification method.

The corresponding ROC curves are shown in Figs. 4–6. Figure 4 shows the ROC curves for differentiating no ptosis from mild ptosis, with expert clinical grading and MRD1-based classification presented in panels A and B, respectively. Figure 5 presents the corresponding ROC curves for differentiating mild from moderate ptosis, while Fig. 6 presents the ROC curves for differentiating moderate from severe ptosis.

Schematic illustrations demonstrating the geometric framework and interpretation of the proposed eyelid contour measurements are provided in Figs. 7–9.

Discussion

The transformation of clinically observed phenotypes into objective, reproducible, and scalable digital biomarkers represents an important goal of digital medicine. (25) Medical imaging provides an opportunity to convert morphological characteristics that are traditionally assessed subjectively into quantitative features suitable for standardized evaluation and computational analysis. (26) In ophthalmology, although digital photography is routinely available in clinical practice, clinically applicable image-derived biomarkers for eyelid disorders remain insufficiently developed.

Interpreting clinical findings into objective quantitative data remains a challenge in ophthalmology. Standardized image-based measurement techniques have the potential to improve the reliability and reproducibility of clinical assessment. Previous studies have employed digital photography and, more recently, deep learning technologies to quantify eyelid morphology, primarily focusing on measurements such as MRD, LMF, upper eyelid crease position, and PFH. (13, 27) Although these parameters are useful for evaluating eyelid position, they provide

limited information regarding eyelid contour, which is an important component of both the functional and cosmetic manifestations of blepharoptosis.

In the present study, we introduced three novel image-derived quantitative indices for evaluating upper eyelid contour: Upper Nasal Index (UNI), Upper Temporal Index (UTI), and Upper Lid Contour Circularity Index (ULCCI)-to characterize upper eyelid morphology. By converting clinically relevant contour features into reproducible numerical measurements, this approach provides a framework for digital phenotyping of blepharoptosis. An important consideration in the development of digital biomarkers is validation against clinically meaningful reference standards. In this study, the proposed indices were evaluated against expert clinical assessment, representing integrated clinical perception of eyelid morphology, and MRD1-based classification, representing a widely accepted quantitative measurement approach. All three indices differed significantly among ptosis severity groups using both classification methods. Importantly, these differences remained significant after adjustment for age and sex, supporting the potential value of these indices as quantitative measures of eyelid morphology independent of these demographic factors.

However, each index demonstrated a distinct pattern across disease severity, suggesting that different aspects of eyelid contour contribute to both objective measurements and clinicians' perception of ptosis.

MRD1 was measured independently by two experienced ophthalmologists using standardized digital photographs. Although MRD1 remains the most widely accepted quantitative measure of ptosis severity, previous studies have demonstrated interobserver variability of up to 0.5 mm.(16) Nevertheless, manual and digital image-based MRD1 measurements have been shown to provide comparable results.(28) In the present study, expert clinical grading demonstrated excellent reliability, with an interobserver ICC of 0.92 and an intraobserver ICC of 0.93. These findings indicate that the clinical grading system used in this study was highly reproducible. Despite this high reliability, the agreement between expert clinical grading and MRD1-based classification was not perfect, suggesting that the two approaches may capture different aspects of eyelid morphology.

The significant correlations observed between MRD1 and all three contour indices further support their relationship with conventional measures of ptosis severity. The strongest association was observed for UTI ($r = 0.811$), followed by UNI ($r = 0.726$) and ULCCI ($r = 0.669$), with all correlations reaching statistical significance ($P < 0.001$). These findings indicate that the proposed indices are related to central eyelid height while also reflecting regional and global characteristics of upper eyelid contour. Importantly, the correlations do not imply that these indices are interchangeable with MRD1, as each capture different geometric characteristics of the upper eyelid.

The distribution of UNI and UTI values across severity categories revealed a distinct cross-sectional pattern of regional upper eyelid contour differences in blepharoptosis. In eyes classified as having no ptosis, UNI and UTI were nearly identical, whereas in the mild ptosis category, UNI was lower than UTI, indicating greater nasal contour alteration relative to the temporal region. In the moderate ptosis category, the two indices became comparable, while in the severe ptosis category, UTI was lower than UNI, indicating greater temporal contour alteration relative to the nasal region. This cross-sectional pattern was observed consistently under both expert clinical grading and MRD1-based classification. Although these findings do not establish a temporal sequence of morphological changes within individual patients, they suggest that the relative contribution of nasal and temporal contour alterations differs across ptosis severity categories.

These findings are consistent with previous quantitative studies demonstrating preferential temporal involvement of the upper eyelid in blepharoptosis. Aytogan and Ayıntap reported greater temporal eyelid drop in unilateral ptosis, with temporal contour symmetry lower than nasal symmetry preoperatively. In their study, the preoperative temporal and nasal degrees of symmetry were 33% and 41%, respectively, and temporal eyelid drop was more pronounced in patients with severe ptosis than in those with mild or moderate ptosis.(12) Similarly, Cruz et al., using computerized image processing to quantify upper eyelid contour, reported that patients with severe congenital blepharoptosis and poor levator function had an almost flat upper eyelid contour with medial displacement of the contour peak and disproportionate lateral drooping, resulting in a reduced temporal-to-nasal upper-quadrant area ratio compared with controls. They concluded that the lateral segment of the upper eyelid was more involved than the nasal segment in congenital blepharoptosis.(23) These observations provide independent support for our finding of greater temporal contour involvement in severe ptosis. In our study, UTI decreased more than UNI in severe ptosis under both expert clinical grading and MRD1-based classification, potentially explaining the superior performance of UTI in distinguishing moderate from severe ptosis. This interpretation is further supported by anatomical studies demonstrating that the lateral horn of the levator aponeurosis is structurally stronger than the medial horn and plays an important role in maintaining the normal curvature of the upper eyelid.(29, 30) The relative preservation of the stronger lateral support may explain why early or mild ptosis may preferentially manifest as nasal contour alteration, whereas more advanced ptosis, when the supporting structures become increasingly compromised, may involve greater temporal eyelid descent.

A fundamental diagnostic challenge in oculoplastic evaluation is reliably differentiating healthy individuals from patients with mild blepharoptosis. Conventional linear metrics, particularly MRD1, evaluate eyelid position solely along a single vertical vector passing through the pupil center. However, early or subtle aponeurotic ptosis frequently manifests not as an isolated central drop, but as focal nasal descent, localized contour flattening, or lateral displacement of the eyelid peak—morphological changes that can easily occur while the central MRD1 remains within normal or borderline limits (3–4 mm). Consequently, single-point height measurements lack the spatial sensitivity required to reliably flag subtle early-stage disease, creating a clinical blind spot in objective diagnostic screening.

In contrast to one-dimensional measurements, expert clinical grading inherently operates as a holistic visual assessment. When an experienced surgeon evaluates an eyelid, their subjective judgment integrates multi-dimensional spatial cues—including the natural parabolic curvature, nasal-to-temporal symmetry, relationship to the superior limbus, and overall facial harmony. Thus, expert clinical grading may capture aspects of eyelid morphology that are not represented by isolated vertical measurements disparity explains why expert impression often diverges from strict MRD1 thresholds, particularly in borderline cases where total eyelid contour, rather than central elevation alone, governs the clinical perception of disease severity.

The novel indices introduced in this study, UNI, UTI, and ULCCI, effectively bridge this gap by digitizing the multidimensional gestalt of expert assessment into objective, highly repeatable metrics. By evaluating regional area ratios rather than unidimensional lengths, these indices quantify structural alterations across the entire upper eyelid margin.

UNI showed particularly good discrimination between no ptosis and mild ptosis, whereas UTI showed particularly good discrimination between moderate and severe ptosis. In severe ptosis, the lower UTI values relative to UNI indicated relatively greater temporal contour alteration, particularly in advanced disease.

An important observation of the present study is that ULCCI demonstrated consistent ability to differentiate adjacent severity groups under expert clinical assessment, whereas it was less effective for distinguishing no ptosis from mild ptosis using MRD1-based classification. Unlike MRD1, which reflects only the central height of the eyelid, expert clinical assessment incorporates the overall appearance of the eyelid, including contour, symmetry, eyelid peak position, and pupil coverage. The consistent performance of ULCCI with expert grading suggests that global eyelid contour characteristics contribute to clinicians' assessment of ptosis severity and may explain, in part, why expert grading does not always correspond exactly with MRD1 measurements. Together with the regional information provided by UNI and UTI, ULCCI provides complementary quantitative information to conventional MRD1 and may have potential utility for standardized clinical documentation, objective severity assessment, and future evaluation of surgical outcomes.

Several previous studies have attempted to quantify eyelid contour in blepharoptosis, thyroid eye disease, aging, and postoperative eyelid evaluation using various geometric measurements.(31, 32) In Graves' orbitopathy, upper eyelid contour abnormalities are characterized by flattening and lateral displacement of the eyelid peak, with greater temporal involvement.(23, 33) Milbratz et al. developed a method based on radial mid-pupil lid distance (MPLD) measurements obtained at 15° intervals across the nasal and temporal eyelid. Their temporal-to-nasal ratio successfully differentiated contour abnormalities, particularly in Graves' disease, and proved useful for optimizing surgical correction of upper eyelid retraction while reducing the risks of overcorrection and undercorrection.(33) Ribeiro et al. similarly quantified upper eyelid contour using mid-pupil eyelid distances before and after surgery in patients with Graves' disease.(34) Lee et al. later applied comparable medial and lateral eyelid measurements to characterize age-related changes in eyelid morphology.(35)

Danesh et al. quantified eyelid contour by measuring vertical distances between the pupil center and the upper eyelid margin at ten points separated by 2-mm intervals. Comparison of external levator resection and Müller's muscle-conjunctival resection demonstrated significant differences at temporal measurement points despite similar postoperative MRD1 values, highlighting the limitations of relying solely on central eyelid height.(14) Equiterio et al. measured marginal reflex distances at multiple lateral eyelid points and demonstrated high sensitivity and specificity for detecting lateral lid flare in Graves' orbitopathy.(36) Bezier curve analysis has also been proposed for quantitative evaluation of eyelid contour and has demonstrated good reproducibility with minimal influence of patient sex.(37) However, Bezier curve analysis may be less suitable for eyes with marked upper eyelid abnormalities because accurate curve fitting becomes increasingly difficult when eyelid morphology is substantially distorted.(38)

Although previous studies have primarily quantified eyelid contour using linear distances or ratios of distances, our approach differs by measuring regional eyelid areas and expressing them as proportions of standardized geometric reference areas. Because area measurements incorporate two-dimensional changes in eyelid morphology rather than a single linear dimension, they may provide greater sensitivity for detecting subtle contour abnormalities. The superior performance of UNI in identifying early ptosis and the complementary performance of UTI and ULCCI across different severity stages support this concept and suggest that area-based analysis provides clinically meaningful information beyond conventional linear measurements.

Limitations

This study has several limitations. Identification of the medial and lateral canthi and determination of palpebral fissure boundaries were performed manually, introducing the possibility of observer-dependent variability. In addition, the study was conducted at a single center with a relatively modest sample size, and larger multicenter studies are needed to validate these findings.

The diagnostic cutoff values for the proposed indices were derived from the same cohort in which their diagnostic performance was evaluated and therefore require validation in independent cohorts. No external validation was performed, and future studies should assess the diagnostic performance and optimal thresholds of the indices in independent and multicenter populations. Furthermore, the repeatability of the proposed quantitative indices themselves was not independently assessed. Future studies should evaluate the intraobserver and interobserver repeatability of the image-processing and contour-tracing procedures.

Because this was a cross-sectional study, the observed differences among severity groups should not be interpreted as definitive evidence of a temporal sequence of contour changes within individual patients. Longitudinal studies are required to determine whether the observed regional differences represent changes that occur during the progression of ptosis.

The study population included a broad age range and encompassed different etiologies of blepharoptosis, including congenital and involutional ptosis. Differences in eyelid anatomy, levator function, and age-related soft tissue changes among these subgroups may influence upper eyelid contour independently of ptosis severity. Although adjustment for age and sex was performed, the relatively limited sample size did not allow for stratified analyses according to ptosis etiology or age group. Future studies with larger cohorts should evaluate the performance of the proposed indices separately in congenital, involutional, and other acquired ptosis subgroups.

In addition, photographic acquisition conditions, including lighting, head position, facial expression, camera positioning, and image quality, may influence eyelid contour measurements and could affect the robustness of the proposed indices under routine clinical conditions. Finally, the single-center study population may limit the generalizability of the findings across different ethnicities, age groups, and etiologies of ptosis. Further validation in larger and more diverse populations is therefore warranted.

Conclusion

In conclusion, this study introduces three quantitative image-derived indices for objective assessment of upper eyelid contour in blepharoptosis. UNI demonstrated the best discriminatory performance for detecting early ptotic changes, whereas UTI showed superior discrimination of advanced disease based on both expert and MRD1 classifications. ULCCI most closely reflected expert clinical grading, suggesting that global eyelid contour is an important determinant of clinicians' perception of ptosis severity. Together, these findings support the complementary use of quantitative eyelid contour analysis alongside conventional MRD1 measurements for the objective assessment and grading of blepharoptosis and provide a foundation for future

automated image-based diagnostic systems.

Declarations

Author Contribution

E.K.P. and Y.S. contributed equally to this work. E.K.P. and Y.S. contributed to study methodology, data curation, formal analysis, and preparation of the original manuscript. They also contributed to manuscript review and editing.H.R.E. contributed to study methodology, data curation, and manuscript writing, review, and editing. T.M. contributed to the design and implementation of the automated algorithm, interpretation of data, and manuscript revision.K.R. contributed to visualization through preparation of Figures 7–9 and contributed to manuscript writing, review, and editing. S.K., K.V., and S.M. contributed to data collection, data preparation, and manuscript review and editing.S.M.R. conceived and designed the study, developed the overall methodology, supervised the project including data curation and formal analysis, administered the project, and contributed to manuscript review and editing.

Tables

Table 1. The demographic characteristics of the participants according to expert classification

MRD1, Margin reflex distance 1; SD, standard deviation. Bold values are statistically significant.

		Group				*P - value*
		Normal	Mild	Moderate	Severe	
Sex	Male	8 (26.7%)	6 (28.6%)	7 (28.0%)	9 (50.0%)	0.337
	Female	22 (73.3%)	15 (71.4%)	18 (72.0%)	9 (50.0%)	
Laterality	Right	13 (43.3%)	8 (38.1%)	12 (48.0%)	10 (55.6%)	0.726
	Left	17 (56.7%)	13 (61.9%)	13 (52.0%)	8 (44.4%)	
Age	Mean ± SD	45 ± 10	33 ± 15	34 ± 11	38 ± 21	<0.001
	Range	25 to 67	3 to 67	16 to 57	4 to 62	
MRD1	Mean ± SD	4.1 ± 0.5	3.2 ± 0.6	2.2 ± 0.4	0.4 ± 1	<0.001
	Range	3.3 to 5	2.1 to 4.4	1.5 to 3.1	-1.4 to 2.2	
MRD1-Fellow eye	Mean ± SD	4.2 ± 0.6	4.1 ± 0.7	4.0 ± 0.7	4.2 ± 1.1	0.782
	Range	2.8 to 5.5	2.8 to 5.5	2.8 to 5.4	1.8 to 6	
MRD1-diff	Mean ± SD	-0.06 ± 0.31	-0.95 ± 0.44	-1.85 ± 0.49	-3.78 ± 1.0	<0.001
	Range	-0.7 to 0.7	-2.1 to -0.2	-2.8 to -0.9	-6.3 to -2.2	

Table 2
Mean values of the evaluated indices according to expert clinical classification with age- and sex-adjusted comparison between groups

Group									
	Normal		Mild		Moderate		Severe		p-value
	Mean±SD	Range	Mean±SD	Range	Mean±SD	Range	Mean±SD	Range	
UNI	0.4273 ± 0.037	0.3556 to 0.5044	0.3794 ± 0.0482	0.2966 to 0.4549	0.3388 ± 0.0363	0.2719 to 0.4145	0.3018 ± 0.0726	0.1858 to 0.4083	< 0.001
UTI	0.4216 ± 0.0553	0.3416 to 0.5709	0.4018 ± 0.0351	0.3331 to 0.4676	0.3347 ± 0.0364	0.2668 to 0.4191	0.2829 ± 0.0691	0.1722 to 0.3666	< 0.001
ULCCI	0.7719 ± 0.0207	0.7318 to 0.8221	0.7620 ± 0.0144	0.7405 to 0.7968	0.7397 ± 0.0134	0.7138 to 0.7789	0.7222 ± 0.0212	0.6914 to 0.7508	< 0.001

Mean values of the Upper Nasal Index (UNI), Upper Temporal Index (UTI), and Upper Lid Contour Circularity Index (ULCCI) according to expert clinical ptosis severity classification. Values are presented as unadjusted mean ± SD. P values were obtained from generalized linear models adjusted for age and sex.

Table 3
Mean values of the evaluated indices according to MRD1 classification with age- and sex-adjusted comparison between groups

Group									
	Normal		Mild		Moderate		Severe		p-value
	Mean±SD	Range	Mean±SD	Range	Mean±SD	Range	Mean±SD	Range	
UNI	0.4389 ± 0.0357	0.3835 to 0.5044	0.3796 ± 0.0428	0.2966 to 0.4427	0.3536 ± 0.0466	0.2719 to 0.4549	0.2907 ± 0.0778	0.1858 to 0.4083	< 0.001
UTI	0.4410 ± 0.0532	0.3532 to 0.5709	0.3904 ± 0.0405	0.3331 to 0.4762	0.3483 ± 0.0419	0.2668 to 0.4236	0.2677 ± 0.0704	0.1722 to 0.3666	< 0.001
ULCCI	0.7750 ± 0.0206	0.7509 to 0.8221	0.7650 ± 0.0180	0.7318 to 0.7968	0.7401 ± 0.0174	0.6915 to 0.7789	0.7252 ± 0.0221	0.6914 to 0.7508	< 0.001

Mean values of the Upper Nasal Index (UNI), Upper Temporal Index (UTI), and Upper Lid Contour Circularity Index (ULCCI) according to MRD1-based ptosis severity classification. Values are presented as unadjusted mean ± SD. P values were obtained from generalized linear models adjusted for age and sex.

Table 4
Age- and sex-adjusted pairwise comparisons of eyelid contour indices across adjacent ptosis severity groups

Classification system	Comparison	UNI, P value	UTI, P value	ULCCI, P value
A. Expert clinical grading	Control vs Mild	< 0.001	0.06	0.032
	Control vs Moderate	< 0.001	< 0.001	< 0.001
	Control vs Severe	< 0.001	< 0.001	< 0.001
	Mild vs Moderate	0.002	< 0.001	< 0.001
	Mild vs Severe	< 0.001	< 0.001	< 0.001
	Moderate vs Severe	0.053	0.005	0.001
B. MRD1-based classification	No ptosis vs Mild	0.001	0.001	0.085
	No ptosis vs Moderate	< 0.001	< 0.001	< 0.001
	No ptosis vs Severe	< 0.001	< 0.001	< 0.001
	Mild vs Moderate	0.024	< 0.001	< 0.001
	Mild vs Severe	< 0.001	< 0.001	< 0.001
	Moderate vs Severe	0.006	< 0.001	0.017

Pairwise comparisons of the Upper Nasal Index (UNI), Upper Temporal Index (UTI), and Upper Lid Contour Circularity Index (ULCCI) between adjacent ptosis severity groups after adjustment for age and sex. P values were obtained from generalized linear models with Sidak-adjusted multiple comparisons. UNI, Upper Nasal Index; UTI, Upper Temporal Index; ULCCI, Upper Lid Contour Circularity Index; MRD1, margin reflex distance 1.

Table 5
Diagnostic performance of eyelid contour indices for discriminating adjacent ptosis severity groups

Severity comparison	Classification method	Index	AUC (95% CI)	Optimal cutoff*	Sensitivity (%)	Specificity (%)
No ptosis vs. mild	Expert clinical grading	UNI	0.768 (0.634–0.902)	0.395	62	87
		UTI	0.606 (0.451–0.762)	0.426	81	47
		ULCCI	0.665 (0.514–0.817)	0.768	71	60
	MRD1-based classification	UNI	0.846 (0.733–0.959)	0.423	88	75
		UTI	0.767 (0.623–0.910)	0.405	75	80
		ULCCI	0.610 (0.443–0.778)	0.765	50	70
Mild vs. moderate	Expert clinical grading	UNI	0.737 (0.587–0.887)	0.382	92	52
		UTI	0.918 (0.836–1.000)	0.362	84	90
		ULCCI	0.882 (0.785–0.979)	0.748	72	90
	MRD1-based classification	UNI	0.656 (0.516–0.797)	0.342	53	79
		UTI	0.765 (0.644–0.886)	0.368	78	71
		ULCCI	0.843 (0.744–0.942)	0.751	75	79
Moderate vs. severe	Expert clinical grading	UNI	0.656 (0.470–0.841)	0.305	56	84
		UTI	0.711 (0.547–0.875)	0.305	56	76
		ULCCI	0.744 (0.582–	0.728	61	92

Severity comparison	Classification method	Index	AUC (95% CI)	Optimal cutoff*	Sensitivity (%)	Specificity (%)
			0.906)			
	MRD1-based classification	UNI	0.752 (0.570–0.934)	0.303	64	89
		UTI	0.817 (0.676–0.959)	0.266	57	100
		ULCCI	0.690 (0.525–0.856)	0.728	50	83

*Optimal cutoff values were determined using the Youden index (sensitivity + specificity − 1). Abbreviations: AUC, area under the receiver operating characteristic curve; CI, confidence interval; MRD1, margin reflex distance 1; UNI, Upper Nasal Index; UTI, Upper Temporal Index; ULCCI, Upper Lid Contour Circularity Index

References

1. Finsterer J. Ptosis: causes, presentation, and management. Aesthetic plastic surgery. 2003;27(3):193–204.
2. Avdagic E, Phelps PO. Eyelid ptosis (Blepharoptosis) for the primary care practitioner. Disease-a-month: DM. 2020;66(10):101040.
3. Heidari M, Haydar AA, Rajabi MT, Rafizadeh SM. Corneal biophysical changes after upper eyelid blepharoplasty and ptosis surgery: a review. BMC ophthalmology. 2023;23(1):253.
4. Savino G, Battendieri R, Riso M, Traina S, Poscia A, D'Amico G, et al. Corneal Topographic Changes After Eyelid Ptosis Surgery. Cornea. 2016;35(4):501–5.
5. Assadi FA, Narayana S, Yadalla D, Rajagopalan J, Joy A. Effect of congenital ptosis correction on corneal topography- A prospective study. Indian journal of ophthalmology. 2021;69(6):1527–30.
6. Dogan AS, Acar M, Kosker M, Arslan N, Gurdal C. Alterations in corneal epithelial thickness in patients with congenital myogenic eyelid ptosis. International ophthalmology. 2018;38(1):53–7.
7. Rafizadeh SM, Sonbolestan SA, Zeidabadinejad H, Abtahi MA. Blepharoptosis and corneal epithelial thickness alterations, is there any relation? BMC ophthalmology. 2024;24(1):282.
8. Aydemir E, Aksoy Aydemir G. Ptosis effects on intraocular lens power calculation. Journal of cataract and refractive surgery. 2023;49(2):171–6.
9. Bagheri A, Tavakoli M, Najmi H, Erfanian Salim R, Yazdani S. Comparison between eyelid indices of ptotic eye and normal fellow eye in patients with unilateral congenital ptosis. Journal of plastic, reconstructive & aesthetic surgery: JPRAS. 2016;69(1):e5-9.
10. Zheng X, Kakizaki H, Goto T, Shiraishi A. Digital Analysis of Eyelid Features and Eyebrow Position Following CO(2) Laser-assisted Blepharoptosis Surgery. Plastic and reconstructive surgery Global open. 2016;4(10):e1063.
11. Small RG, Sabates NR, Burrows D. The measurement and definition of ptosis. Ophthalmic plastic and reconstructive surgery. 1989;5(3):171–5.

12. Aytogan H, Ayıntap E. Comparing the symmetry of upper eyelid following unilateral ptosis correction. BMC ophthalmology. 2021;21(1):438.
13. Mahmoudi T, Riazi-Esfahani H, Montazeriani Z, Yaseri M, Mehdipour Namdar Z, Jamali M, et al. Sector area index: a novel supporting marker for blepharoptosis screening and grading. International ophthalmology. 2023;43(12):4967–78.
14. Danesh J, Ugradar S, Goldberg R, Rootman DB. A novel technique for the measurement of eyelid contour to compare outcomes following Muller's muscle-conjunctival resection and external levator resection surgery. Eye (London, England). 2018;32(9):1493–7.
15. Khalili Pour E, Mahmoudi T, Ahmadzadeh H, Rafizadeh SM, Riazi-Esfahani H. Quantitative analysis of the eyelid curvature in patients with blepharoptosis. BMC medical imaging. 2024;24(1):97.
16. Boboridis K, Assi A, Indar A, Bunce C, Tyers AG. Repeatability and reproducibility of upper eyelid measurements. The British journal of ophthalmology. 2001;85(1):99–101.
17. Hwang K, Ko YS. Improvement of the Marginal Reflex Distance-1 in Blepharoptosis Surgeries. The Journal of craniofacial surgery. 2016;27(2):455–60.
18. Soleymanzadeh M, Esmaili K, Rafizadeh SM. A novel technique for small-incision levator resection with a double mattress suture for ptosis correction. Graefe's archive for clinical and experimental ophthalmology = Albrecht von Graefes Archiv fur klinische und experimentelle Ophthalmologie. 2023;261(12):3607–13.
19. Sendul SY, Atilgan CU, Dirim B, Yildiz AM, Arslan GD, Demir ST, et al. The Effect of Two Different Frontalis Sling Approaches on Postoperative Eyelid Contour: A Comparative Study. Aesthetic plastic surgery. 2020;44(2):381–9.
20. Ahn S, Lee H, Lee J, Park J, Park M, Baek S. Analysis of Surgical Outcome After Levator Advancement by Assessing Changes in Eyelid Contour. The Journal of craniofacial surgery. 2016;27(5):1147–50.
21. Mocan MC, Ilhan H, Gurcay H, Dikmetas O, Karabulut E, Erdener U, et al. The expression and comparison of healthy and ptotic upper eyelid contours using a polynomial mathematical function. Current eye research. 2014;39(6):553–60.
22. Akaishi P, Galindo-Ferreiro A, Cruz AAV. Symmetry of Upper Eyelid Contour After Unilateral Blepharoptosis Repair With a Single-strip Frontalis Suspension Technique. Ophthalmic plastic and reconstructive surgery. 2018;34(5):436–9.
23. Cruz AA, Coelho RP, Baccega A, Lucchezi MC, Souza AD, Ruiz EE. Digital image processing measurement of the upper eyelid contour in Graves disease and congenital blepharoptosis. Ophthalmology. 1998;105(5):913–8.
24. Gower EW, West SK, Cassard SD, Munoz BE, Harding JC, Merbs SL. Definitions and standardization of a new grading scheme for eyelid contour abnormalities after trichiasis surgery. PLoS neglected tropical diseases. 2012;6(6):e1713.
25. Coravos A, Khozin S, Mandl KD. Developing and adopting safe and effective digital biomarkers to improve patient outcomes. NPJ digital medicine. 2019;2(1).
26. Gillies RJ, Kinahan PE, Hricak H. Radiomics: Images Are More than Pictures, They Are Data. Radiology. 2016;278(2):563–77.
27. Coombes AG, Sethi CS, Kirkpatrick WN, Waterhouse N, Kelly MH, Joshi N. A standardized digital photography system with computerized eyelid measurement analysis. Plastic and reconstructive surgery. 2007;120(3):647–56.

28. Lou L, Yang L, Ye X, Zhu Y, Wang S, Sun L, et al. A Novel Approach for Automated Eyelid Measurements in Blepharoptosis Using Digital Image Analysis. Current eye research. 2019;44(10):1075–9.
29. Kakizaki H, Malhotra R, Selva D. Upper eyelid anatomy: an update. Annals of plastic surgery. 2009;63(3):336–43.
30. Ettl A, Priglinger S, Kramer J, Koornneef L. Functional anatomy of the levator palpebrae superioris muscle and its connective tissue system. The British journal of ophthalmology. 1996;80(8):702–7.
31. Mak FH, Harker A, Kwon KA, Edirisinghe M, Rose GE, Murta F, et al. Analysis of blink dynamics in patients with blepharoptosis. Journal of the Royal Society, Interface. 2016;13(116).
32. Lou L, Cao J, Wang Y, Gao Z, Jin K, Xu Z, et al. Deep learning-based image analysis for automated measurement of eyelid morphology before and after blepharoptosis surgery. Annals of medicine. 2021;53(1):2278–85.
33. Milbratz GH, Garcia DM, Guimarães FC, Cruz AA. Multiple radial midpupil lid distances: a simple method for lid contour analysis. Ophthalmology. 2012;119(3):625–8.
34. Ribeiro SF, Milbratz GH, Garcia DM, Devoto M, Guilherme Neto H, Mörschbächer R, et al. Pre- and postoperative quantitative analysis of contour abnormalities in Graves upper eyelid retraction. Ophthalmic plastic and reconstructive surgery. 2012;28(6):429–33.
35. Lee H, Lee JS, Chang M, Park M, Baek S. Analysis of lid contour change with aging in Asians by measuring midpupil lid distance. Plastic and reconstructive surgery. 2014;134(4):521e-9e.
36. Equiterio BS, Garcia DM, Cruz AA, Rootman DB, Goldberg RA, Sales-Sanz M, et al. Lid Flare Measurement with Lateral Midpupil Distances. Current eye research. 2021;46(9):1309–13.
37. Golbert MB, Garcia DM, Akaishi PMS, Cruz A. Upper eyelid contour symmetry measurement with Bézier curves. Arquivos brasileiros de oftalmologia. 2020;83(1):28–32.
38. Huelin FJ, Sales-Sanz M, Ye-Zhu C, Cruz AAV, Muñoz-Negrete FJ, Rebolleda G. Bézier curves as a total approach to measure the upper lid contour: redefining clinical outcomes in palpebral surgery. The British journal of ophthalmology. 2023;107(1):6–11.

Figures

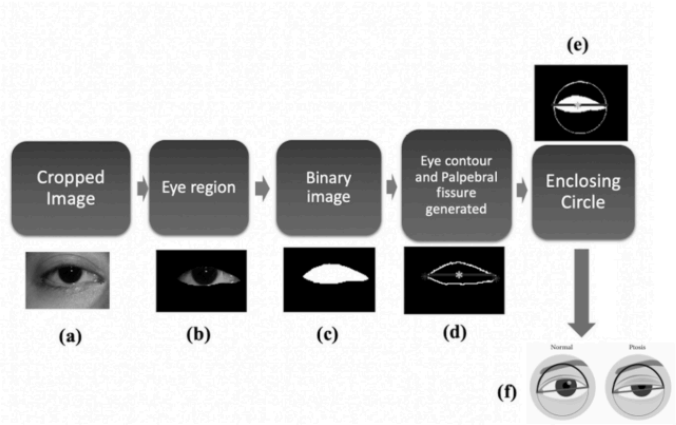


Figure 1

Example of preprocessing a digital photograph for deriving measured indices. The images were converted to grayscale (a). On the image, the operator has marked the medial and lateral canthi (b). To build a palpebral fissure region of interest (ROI) with an interactive polygonal drawing approach, the operator would first click on the medial or lateral canthus, then drag the mouse along the eyelid contour, and then click on the opposite canthus (c). The image was then binarized, and a circle was formed around the eye, with the connecting line between the medial and lateral canthi serving as the diameter (d, e). Schematic examples of preprocessed images of a normal and ptotic eye (f).

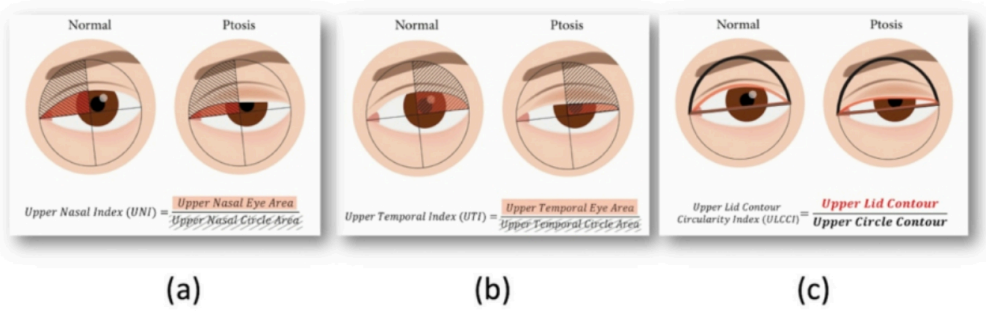


Figure 2

We formed an imaginary circle using the line between lateral and medial canthi as its diameter to determine the indices. As shown in Figure 2a, the Upper Nasal Index (UNI) was calculated by dividing the area confined between the upper eyelid margin and the imaginary circle's diameter (the line between medial and lateral canthi) by the upper half of the imaginary circle in the nasal side (to define the nasal side, we drew a perpendicular line at the midpoint). Second was the Upper Temporal Index. Figure 2b shows UTI determined using the same method as UNI in the temporal eye. The study also revealed upper Lid Contour Circularity Index (ULCCI). Figure 2c shows how to construct this index by dividing the length of the upper lid contour by the circumference of the upper half of the circle.

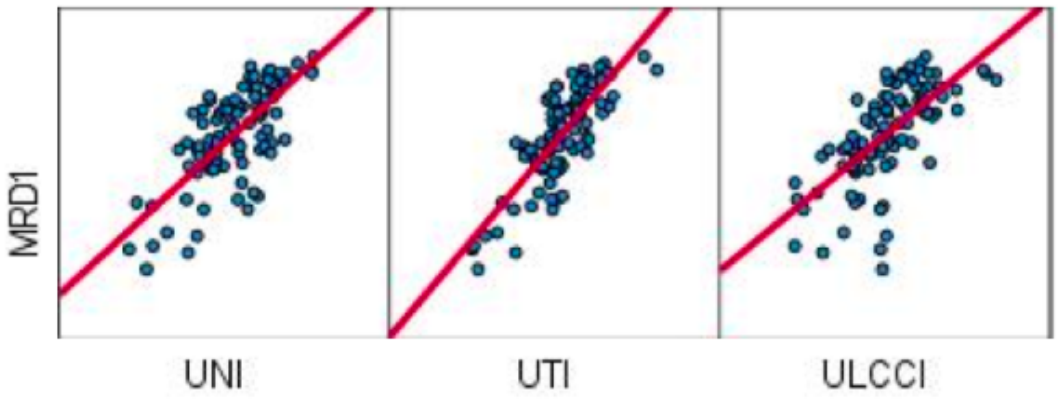


Figure 3

Scatterplot matrix showing the relationships between Margin Reflex Distance 1 (MRD1) and the Upper Nasal Index (UNI), Upper Temporal Index (UTI), and Upper Lid Contour Circularity Index (ULCCI). Each panel displays individual observations with a fitted linear regression trendline (red line), illustrating the relationship between MRD1 and the corresponding eyelid contour index.

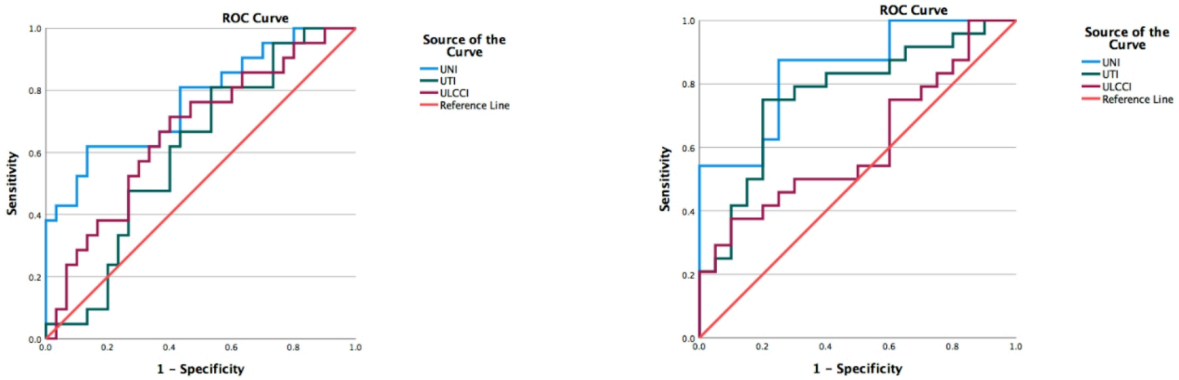


Figure 4

Receiver operating characteristic curves for differentiation of no ptosis and mild ptosis. (a) ROC curves for the Upper Nasal Index (UNI), Upper Temporal Index (UTI), and Upper Lid Contour Circularity Index (ULCCI) based on expert clinical grading. (b) Corresponding ROC curves based on MRD1-based classification.

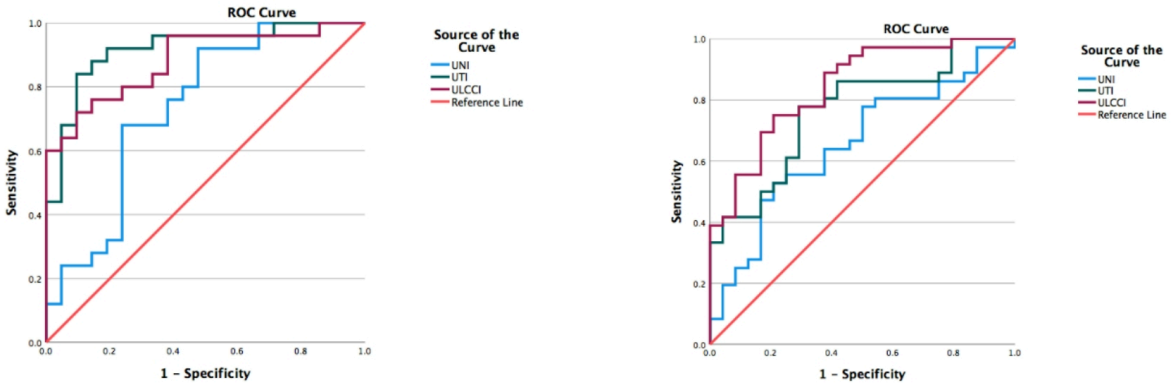


Figure 5

Receiver operating characteristic curves for differentiation of mild and moderate ptosis. (a) ROC curves for UNI, UTI, and ULCCI based on expert clinical grading. (b) Corresponding ROC curves based on MRD1-based classification.

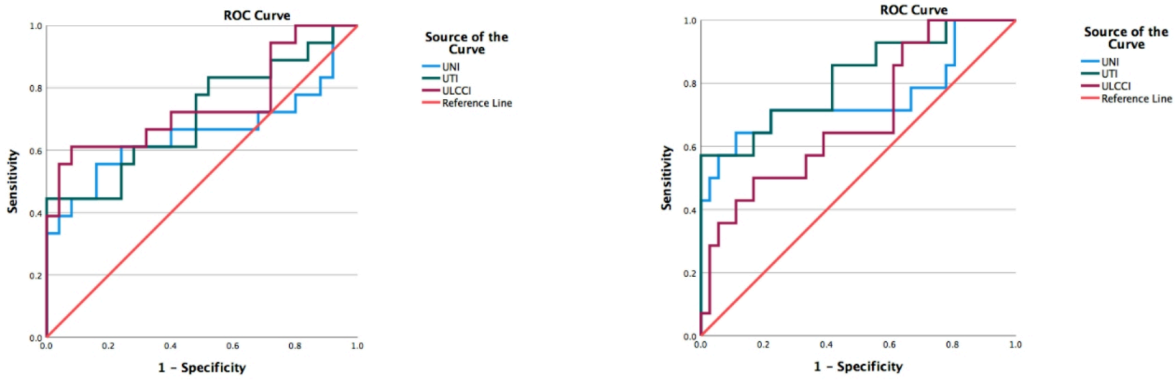


Figure 6

Receiver operating characteristic curves for differentiation of moderate and severe ptosis. (a) ROC curves for UNI, UTI, and ULCCI based on expert clinical grading. (b) Corresponding ROC curves based on MRD1-based classification.

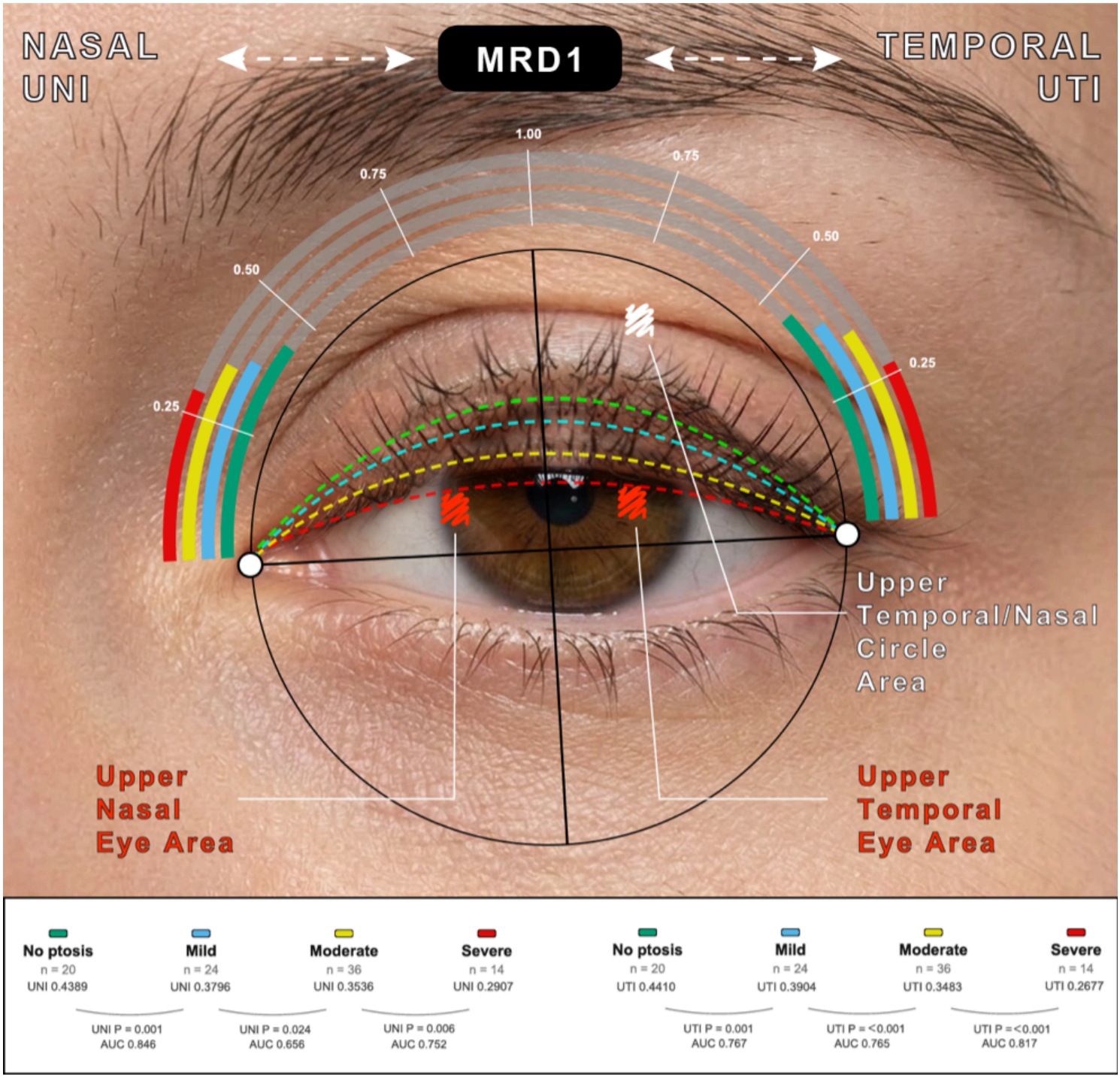


Figure 7

UNI and UTI by MRD1-based ptosis severity. The circle is drawn on the intercanthal line (white markers) as its diameter and split by the perpendicular through its midpoint; UNI is the upper nasal eye area (red hatched key) divided by the upper nasal quadrant area (white hatched key), and UTI is the same in the temporal quadrant. Dashed lines are reconstructed eyelid margins reproducing the group means (green, no ptosis; blue, mild; yellow, moderate; red, severe); arcs outside the circle show each mean as a share of its quadrant. Boxes give the number of eyes, the mean, the Sidak-adjusted P value and AUC versus the preceding group. AUC, area under the receiver operating characteristic curve; MRD1, margin reflex distance 1; UNI, Upper Nasal Index; UTI, Upper Temporal Index.

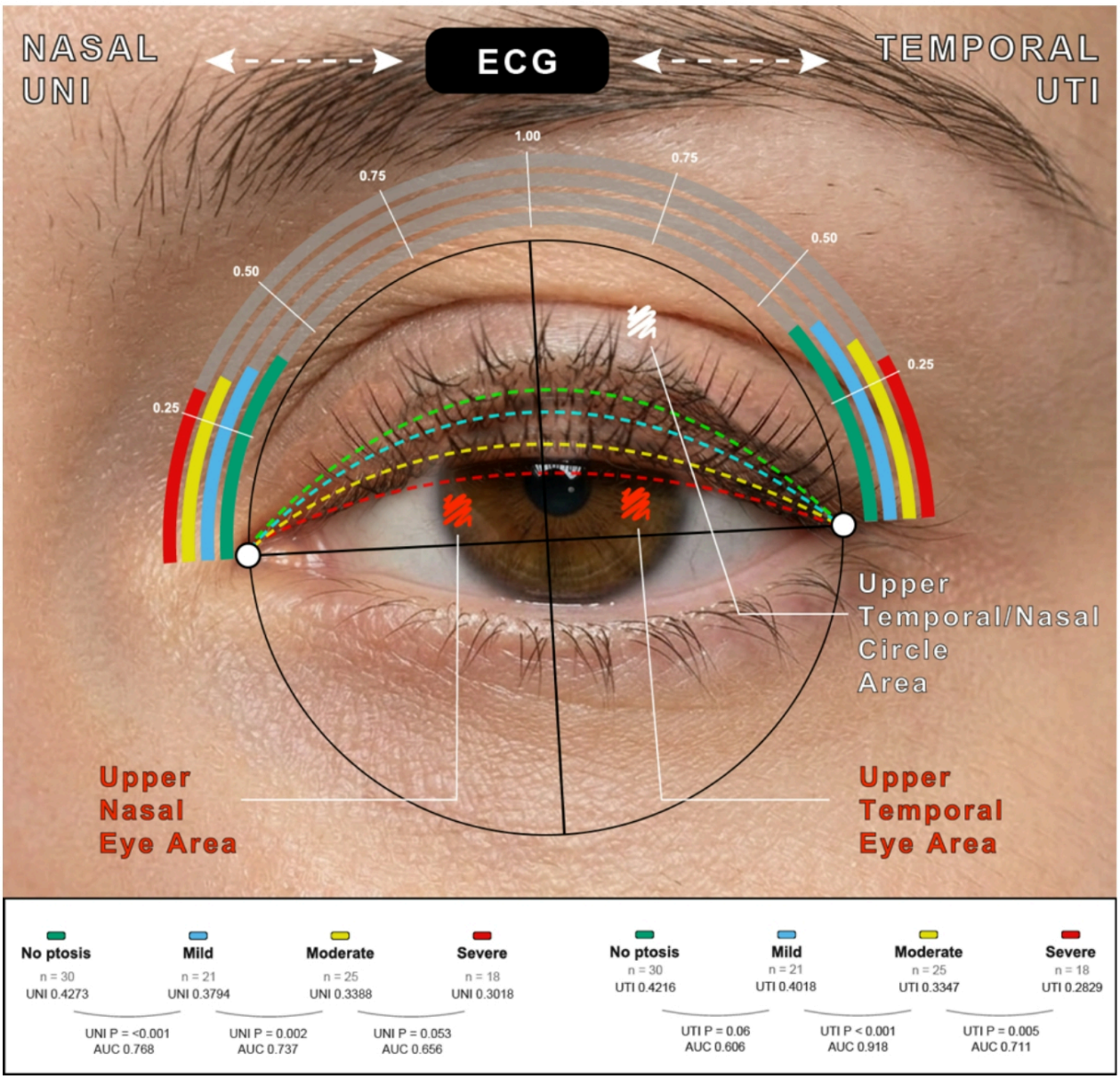


Figure 8

UNI and UTI by expert clinical grading. Construction and keys as in Figure 1, with the expert classification and its values; *P*≥ 0.05 marks the only adjacent comparison that was not significant after Sidak adjustment (UTI, no ptosis versus mild). AUC, area under the receiver operating characteristic curve; ECG, expert clinical grading; UNI, Upper Nasal Index; UTI, Upper Temporal Index.

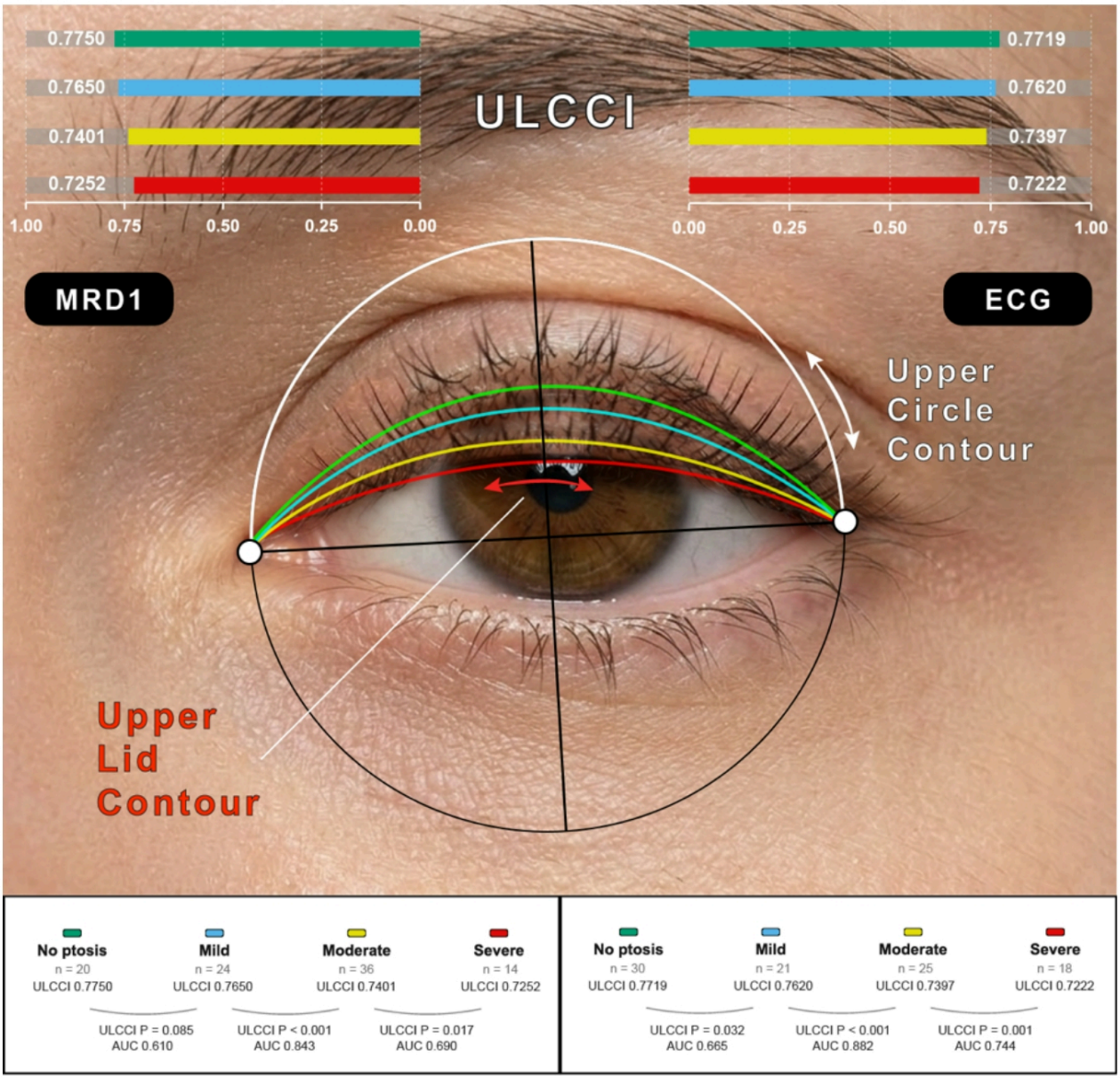


Figure 9

ULCCI by MRD1-based and expert clinical grading severity. ULCCI is the length of the upper eyelid contour (colored lines) divided by the circumference of the upper half of the same circle (white arc). Bars show the group means from 0 to 1, MRD1 on the left and expert grading on the right. Boxes give the number of eyes, the mean, the Sidak-adjusted *P* value and AUC versus the preceding group. AUC, area under the receiver operating characteristic curve; ECG, expert clinical grading; MRD1, margin reflex distance 1; ULCCI, Upper Lid Contour Circularity Index.

Supplementary Files

This is a list of supplementary files associated with this preprint. Click to download.

- SupplementaryTable1.docx